Analysis and Design of Capacitive Parametric Ultrasonic Transducers for Efficient Ultrasonic Power Transfer Based on a 1D Lumped Model

Sushruta Surappa, Molei Tao, and F. Levent Degertekin, *Senior Member, IEEE*

***Abstract*— There is an increasing interest in wireless power transfer for medical implants, sensors networks and consumer electronics. A passive capacitive parametric ultrasonic transducer (CPUT) can be suitable for these application as it does not require a DC bias or permanent charge. In this paper, we present a 1-dimensional lumped parameter model of the CPUT to study its operation and investigate relevant design parameters for power transfer applications. The CPUT is modeled as an ultrasound driven piston coupled to an RLC resonator resulting in a system of two coupled nonlinear ordinary differential equations. Simulink is used along with an analytical approximation of the system to obtain the voltage across the capacitor and displacement of the piston. Parametric resonance threshold and ultrasound to electrical conversion efficiency are evaluated and the dependence of these performance metrics on the load resistance, input ultrasound intensity, forcing frequency, electrode coverage area, gap height and the mechanical Q-factor are studied. Based on this analysis, design guidelines are proposed for highly efficient power transfer. Guided by these results, practical device designs are obtained through COMSOL simulations. Finally, the feasibility of using the CPUT in air is predicted to set the foundation for further research in ultrasonic wireless power transfer, energy harvesting and sensing.**

***Index Terms*— Airborne ultrasound, capacitive parametric ultrasonic transducer (CPUT), non-linear acoustics, parametric resonance, ultrasound transducer, wireless power transfer**

I. Introduction

Ultrasonic transducers have been in use for many years for various applications such as medical imaging, non-destructive testing, wireless power transfer, and as sensors. Almost all ultrasonic transducers can be classified as either piezoelectric transducers or capacitive transducers. Early ultrasound transducers consisted of either a piezoelectric ceramic or a composite array consisting of a number of piezoelectric elements and was used for medical imaging, non-destructive testing (NDT) and as ultrasonic motors amongst many other applications [1]-[4] . With the emergence of micromachining technologies in the 90's, capacitive micro-machined ultrasonic transducers or CMUTs gained increasing prominence for applications such as, intravascular ultrasound imaging (IVUS), tissue harmonic imaging and focused ultrasound [5]–[8]. More recently, there is a strong focus on developing piezoelectric micro-machined ultrasound transducers or PMUTs for fingerprint detection and imaging [9]–[11]. Compared to traditional piezoelectric transducers, PMUTs and CMUTs have the advantage of a miniaturization, a larger bandwidth in immersion and easier electronics integration [12]. This makes them highly suitable for applications such as IVUS and fingerprint sensing, where a large number of elements are required in a small form factor.

Wireless power transfer has recently gained renewed interest with the emergence of implantable medical devices, internet of things (IoT) and wearable technologies [13]–[16]. Despite the integration advantages of CMUTs, so far piezoelectric transducers are used almost exclusively as receivers for ultrasonic wireless power transfer [17]–[19]. This is because the piezoelectric transducer is a completely passive, self-generating device, whereas a DC bias or some permanent charge is required to operate capacitive transducers [20], [21]. This makes capacitive transducers less desirable for wireless power transfer and energy harvesting applications, where a passive system is preferred. Recently, we demonstrated the operation of a new type of parametric resonance based transducer called the capacitive parametric ultrasound transducer or CPUT to overcome these limitations [22]. Unlike direct resonance (where a system is forced at its natural frequency), an electrical or mechanical system can be driven into parametric resonance by varying an internal system parameter such as the reactance or resistance at approximately two times the natural frequency of the system to generate oscillations of large amplitude. This effect has been observed in simple contraptions such as the playground swing [23] as well as in complex vibration energy harvesters [24], [25]. The CPUT consists of a time-varying membrane-based capacitor which forms part of an RLC circuit. By exciting the membrane with ultrasound at two times the resonance frequency of the RLC circuit, we can drive the system into parametric resonance and convert the acoustic energy to electrical energy in a highly efficient manner. Depending on the application, the source of the ultrasound excitation could either be an ultrasound transducer (wireless power) or base excitations (energy harvesting). Unlike conventional capacitive transducers the CPUT can potentially

S. Surappa is with the Woodruff School of Mechanical Engineering, Georgia Institute of Technology, Atlanta, GA (e-mail: sushsurappa@gatech.edu).

M. Tao is with the School of Mathematics, Georgia Institute of Technology, Atlanta, GA (e-mail: mtao@gatech.edu).

F.L Degertekin is with the Woodruff School of Mechanical Engineering, Georgia Institute of Technology, Atlanta, GA (e-mail: levent.degertekin@me.gatech.edu).

start with the help of thermal noise and can be operated without a pre-charged membrane or a DC bias.

In our previous work, a simple model and a demonstration experiment was reported. Parametric resonance is a highly non-linear phenomenon and hence a detailed analysis is required while designing the CPUT in order to achieve optimal operation and performance. In this paper, a 1-dimensional (1D) model of the CPUT is presented and its operational characteristics are explored using Simulink (The MathWorks, Inc., Natick, MA). An alternate, analytical approach to the CPUT problem is also presented, to obtain certain important parameters which provide further insight into CPUT operation. With the help of these two methods of solution, the performance of the CPUT is studied by varying different operational parameters and some practical designs for highly efficient operation in water are simulated in COMSOL. The feasibility of using the CPUT for in-air applications is also discussed in some detail followed by the concluding remarks.

II. Modelling

A. 1-dimensional (1D) model formulation

Unlike many ultrasonic transducers which are typically operated in the linear regime, the CPUT is more complex due to the inherent non-linearities present in the system. Performance parameters such as the acousto-electrical conversion efficiency are strongly dependent on factors such as the medium in which the device is operated, level and frequency of forcing, receiver dynamics and load resistance. Hence it is necessary to carefully consider these factors while designing the CPUT for a particular application.

The CPUT can be considered as a black-box composed of a mechanical domain and an electrical domain. The mechanical domain consists of a time-varying capacitor that is excited by an incident ultrasound field in a fluid. This capacitor is connected in series with an inductor and resistor to form a resonant RLC circuit in the electrical domain. When the capacitance is varied above a certain threshold at around two times the resonance frequency of the RLC circuit, the system is driven into parametric resonance. At this time, a growing current develops across the circuit until it is limited to a steady state value determined by the non-linearities and damping present in the system. Hence the incident acoustic power is converted by the CPUT into electrical power that is then harnessed across the load resistance.

In order to understand its operation, the CPUT is modelled as a 1-dimensional (1D) lumped parameter system as shown in fig. 1. The capacitor is represented as a parallel plate piston with known mass m, stiffness k and damping b in the 1D model. The mass and stiffness values correspond to the equivalent mass and stiffness of a fluid loaded piston capacitor. The damping represents the radiation losses in the fluid and other mechanical damping in the system in this 1D setting. It is assumed here that the mechanical losses in the capacitor are negligible when compared to the fluid losses and is hence ignored. The radiation loss is represented by the real part of the radiation impedance of a circular baffled piston [26] i.e. b=real$\{Z_{fluid}\}$=real$\{R_f+jX_f\}$. The imaginary part of this radiation impedance (which manifests itself through an additional mass loading $X_f=\omega m_f$) can be lumped with the mass of the piston m_0 to obtain the equivalent mass m i.e. $m_0+m_f=m$.

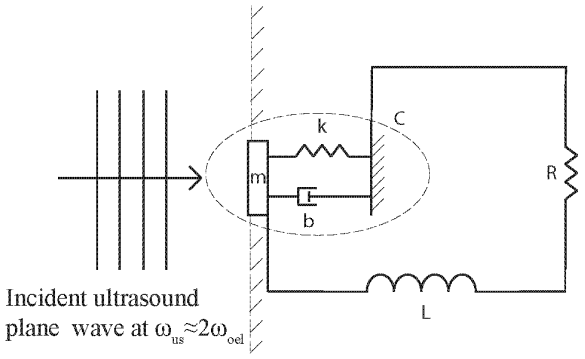

Fig. 1. 1D lumped parameter representation of the CPUT. The mechanical piston consisting of a spring, mass and damper also behaves as a parallel plate capacitor to complete an RLC circuit in the electrical domain.

The incident harmonic ultrasound forcing F_0 at frequency ω_{us} causes the piston to oscillate with a velocity v. In order to maximize the displacement x of the piston ($x=v/j\omega$), the parameters k and m can be chosen such that the resonance frequency of the parallel plate piston is equal to the ultrasound forcing frequency. We shall henceforth call this the mechanical resonance frequency ω_{om}, where

$$\omega_{om} = \sqrt{\frac{k}{m}} \tag{1}$$

We also define the mechanical quality factor of the oscillating piston as

$$Q_m = \frac{\omega_{om} m}{b} \tag{2}$$

The same parallel plate piston also acts as a time-varying capacitor having a capacitance

$$C = \frac{\epsilon_0 A}{d_0 - x} \tag{3}$$

where d_0 is the undisturbed gap between the two plates. This capacitor forms part of the electrical oscillator along with an inductance L and load resistance R. For efficient parametric excitation, the value of the inductor can be chosen such that the resonant frequency of the RLC circuit is approximately half of that of the ultrasound forcing ie. $\omega_{us} \cong 2\omega_{oel}$. Here, ω_{oel} is the resonant frequency of the RLC circuit and is given by,

$$\omega_{oel} = \sqrt{\frac{1}{LC_0}} \tag{4}$$

Where C_0 is the undisturbed capacitance. Similar to eqn. 2, we can define the electrical quality factor of the RLC circuit, Q_{el} as

$$Q_{el} = \frac{\omega_{oel} L}{R} \tag{5}$$

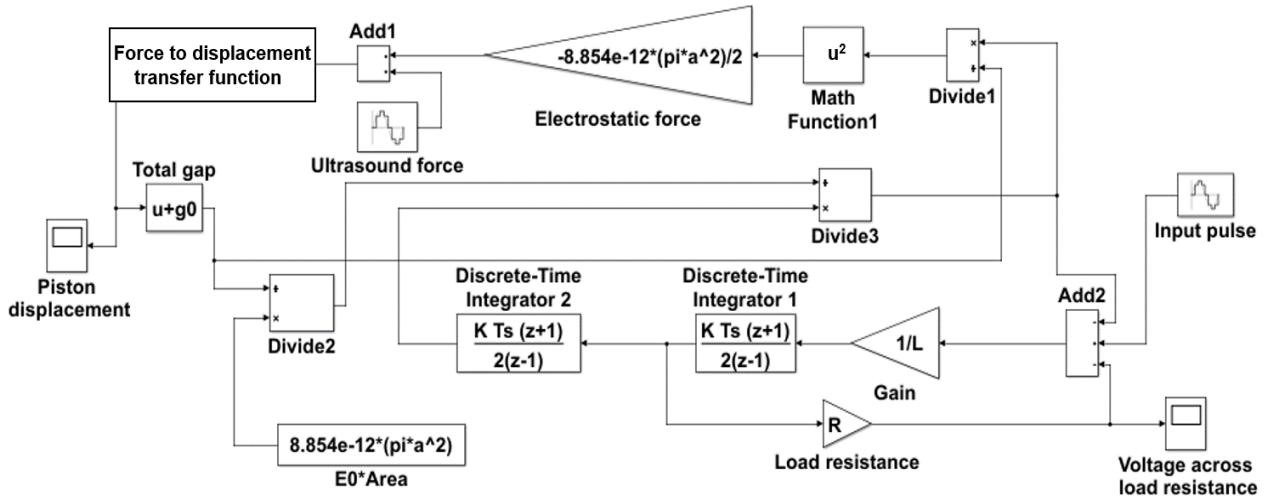

Fig. 2. Simulink block diagram of 1-D CPUT model. The voltage across the resistor and the piston displacement is recorded using a Simulink scope. Information regarding the mass, stiffness and the losses in the piston is included in the force to displacement transfer function block. A gain of 1 and a sampling time of 25 ns is used in the discrete time integrator block.

B. *Mathematical formulation*

The 1D lumped parameter system can also be expressed mathematically as a mechanical oscillator coupled to an electrical oscillator via a time-varying piston capacitor. This can be represented by two coupled non-linear ordinary differential equations:

$$\left[\frac{d^2}{dt^2}+\frac{R}{L}\frac{d}{dt}+\frac{d_0-x}{LA\varepsilon_0}\right]V=0 \tag{6}$$

$$\left[\frac{d^2}{dt^2}+\frac{b}{m}\frac{d}{dt}+\frac{k}{m}\right]x=\frac{F_0}{m}\sin(\omega_{us}t)+\frac{\varepsilon_0 A}{2m}\frac{V^2}{(d_0-x)^2} \tag{7}$$

where the voltage across the capacitor V and displacement of the piston x are the unknowns. The right-hand side of eqn. 7 represents the force acting on the piston and it is the sum of the ultrasound forcing F_0 and the electrostatic force due to the voltage across the capacitor. This system is more complex than the parametric resonance prototype of Mathieu's equation[1], as well as the energy harvesters described in [26], [27], in the sense that it is 4 dimensional ODE system instead of 2. The complexity arises from the fact that the two oscillators are nonlinearly coupled and the displacement of the piston is a function of both external forcing and the voltage generated due to this parametric excitation. The methods of solution for the two formulations are described in the following subsections.

C. *Simulink as a method of solution for the 1D model*

The transient response of the 1D lumped system is analyzed in Simulink by creating a best-form mathematical model of the RLC circuit. In this case, the time-varying capacitor is represented by a block containing a transfer function that takes the voltage across the capacitor and the ultrasound force as the input and provides the parallel piston displacement as the output. The displacement can then be used to determine the instantaneous capacitance, thereby forming a closed loop - this circuit implementation is shown in fig. 2. To provide the necessary initial condition for parametric resonance, an electrical excitation of frequency ω_{oel} is produced in the RLC circuit by providing a short input voltage pulse. This is followed by applying a uniform ultrasound force on the face of the piston at ω_{us}. If the level of forcing exceeds a required threshold, the CPUT is driven into parametric resonance and parameters such as the voltage, current and displacement can be recorded using the Simulink scope. It must be noted that a constant noise source can also be used in place of the voltage pulse to demonstrate that the CPUT can work with only thermo-mechanical noise present.

D. *Analytical solution to the mathematical formulation*

The transient Simulink simulations can be time consuming and non-intuitive when performing an extensive parametric analysis. Accurate analytical approximate solutions can be obtained by careful asymptotic analysis of the coupled non-linear ODEs. These analytical solutions, when used in conjecture with Simulink, provide more insight into CPUT operation by providing expressions for steady state voltage and

[1] Note in Mathieu's equation there is a possibility of losing energy while being parametrically excited (see e.g. [27]), but that will not happen in the system proposed here (see [28]).

displacement amplitudes on the capacitor and the force threshold for parametric resonance. These expressions can provide guidelines on the operational limits of the CPUT without having to simulate a large number of cases using Simulink.

In order to employ asymptotic analysis and simplify notations, the following normalized parameters are introduced:

$$\epsilon = \frac{\mu^3 \varepsilon_0 A}{2m\xi^2},\ \gamma = \frac{R}{L\xi\epsilon},\ \ \alpha = \frac{1}{LA\varepsilon_0\xi^2\mu\epsilon},\ \beta = \frac{b}{m\xi\epsilon}, F = \frac{\mu_0 F_0}{m\xi^2\epsilon},$$
$$D = \mu d_0,\ \omega = \frac{\omega_{0el}}{\xi}$$

where $\boldsymbol{\xi}$=10^7 and μ=10^8 for experimental parameters considered in this article. As a result, $\epsilon \ll 1$ and then a nonstandard coordinate transformation is used to separate the timescales in the system to allow a more accurate approximation via the averaging theory [29]. The details of the method employed to obtain the approximate solutions is explained in [28]. At steady state, the voltage amplitude V across the capacitor, oscillation amplitude of piston displacement r, and average piston displacement y are found to be:

$$V \approx \sqrt{\frac{-8D^4\alpha\beta\gamma\omega^4 + 2D^3\omega\sqrt{N}}{D^2\alpha^2\omega^2 + 16\gamma^2\omega^4 + 4\alpha\beta\gamma D\epsilon\omega^2 + \alpha^2\beta^2\epsilon^2 D^2}} \tag{8}$$

where,

$$N = D^2F^2\alpha^4\omega^2 + 16F^2\alpha^2\gamma^2\omega^4 - 256\beta^2\gamma^4\omega^8 + 4\alpha\beta\gamma D\omega^2(\alpha^2F^2 - 16\beta^2\gamma^2\omega^4)\epsilon + (D^2F^2\alpha^4\beta^2 - 16D^2\alpha^2\beta^4\gamma^2\omega^4)\epsilon^2$$

$$r \approx \sqrt{\left(\frac{2\gamma\omega}{\alpha}\right)^2 + \left(\frac{\epsilon V^2}{4D^2\omega^2}\right)^2} \tag{9}$$

$$y \approx \frac{\epsilon V^2}{8D^2\omega^2} \tag{10}$$

Note if shorter expressions are preferred, V can be further approximated by

$$V \approx \sqrt{\frac{-8D^4\alpha\beta\gamma\omega^2 + 2D^3\sqrt{D^2F^2\alpha^4 + 16F^2\alpha^2\gamma^2\omega^2 - 256\beta^2\gamma^4\omega^6}}{D^2\alpha^2 + 16\gamma^2\omega^2}} \tag{11}$$

since $\epsilon \ll 1$.

As mentioned earlier, due to the resistive losses in the system, in order to drive the electrical circuit into parametric resonance, the change in capacitance must exceed a certain minimum threshold value. The minimum force required to obtain a finite steady state voltage is

$$|F| \geq \frac{4\omega^2}{\alpha}\sqrt{\gamma^2 + 4\Delta^2\omega^2}\sqrt{\beta^2 + 16\Delta^2\omega^2} \tag{12}$$
in particular, if Δ=0, $F_0 \geq 4{\omega_{oel}}^2 RbA\varepsilon_0$

where Δ is the measure of deviation of the forcing frequency from 2ω. It is assumed that the radiation impedance seen by the piston remains constant in this Δ interval. From eqn. 12 it is observed that if Δ=0, F_0 depends only on b, R, ω_{oel} and A. In our 1D model, b purely depends on the medium of operation – this implies that a lower minimum force is required to operate in a fluid having a lower acoustic impedance. Similarly, operating the CPUT at a lower frequency also reduces the forcing required for parametric excitation. The effect of reducing b and ω_{oel} is studied in greater detail in section IV, where the feasibility of operating CPUT in air is explored. The CPUT is also very sensitive to a small input force if the load resistance R and electrode area A is reduced. While this may not be practical for power transfer, where there is an optimum value of load resistance at which the impedance is matched, it may be more feasible in sensing applications, where impedance matching is not an issue and load resistance can be minimized to achieve high force sensitivity.

III. Results

The above formulations allow one to investigate the performance of CPUTs for power transfer applications which depends on both electrical and mechanical parameters. For this purpose, in this section we define the relevant performance metrics and analyze the results for a specific CPUT operating around 2 MHz in immersion.

A. Parametric study using an example CPUT

As an example, a CPUT with parameters listed in table 1 is used to explore the device characteristics using the two models developed. Assuming that the CPUT is operated inside the human body for wireless powering of implantables, water is chosen as the medium of operation as it closely mimics the acoustic properties of human tissue. An ultrasound frequency of 2 MHz and a piston area of 1mm^2 is chosen such that the device has a small footprint and can be operated at a reasonable depth inside water. The values of k and m are chosen such that the mechanical resonance frequency is always 2 MHz and the value of the inductance is chosen such that the electrical resonance frequency is always 1MHz. It must also be noted that although the input ultrasound intensity is varied between 1mW/mm^2 and 15 mW/mm^2 for the sake of simulations, the maximum FDA permissible limit of diagnostic ultrasound is 7.2mW/mm^2 [30].

TABLE I
PARAMETERS USED FOR EXAMPLE CPUT

Symbol	Quantity	Value
A	Piston area	1 mm^2
k	Piston stiffness	1×10^8 N/m
m_0	Piston mass	6.12×10^{-7} kg
d_0	Vacuum gap	120 nm
ω_{us}	Ultrasound frequency	2 MHz
ω_{oem}	Mechanical resonance frequency	2 MHz
ω_{oel}	Electrical resonance frequency	1 MHz

An important figure of merit to evaluate the transducer for power transfer applications is the efficiency of the CPUT. Using Simulink, the efficiency can be calculated as the ratio of

the time averaged power dissipated across the resistor to the available acoustic power.

$$efficiency = \frac{\frac{1}{T}\int i^2 R\, dt}{Available\ power} \times 100(\%) \quad (13)$$

Here, i is the current in the circuit and R is the load resistance. The available power is given by $(p.A)^2/R_f$, where p is the rms pressure on the face of the piston under perfectly matched impedance conditions, A is the area of the piston and R_f is the radiation resistance. To be consistent, we assume that this pressure is generated by an incident acoustic wave of intensity $I=p^2.A/R_f$.

When the CPUT input impedance is well matched with the acoustic impedance of the fluid, most of the acoustic energy incident on the piston passes through with minimal reflection and is available across the load resistance as electrical power. Hence one way of achieving high efficiency is to minimize the power reflection coefficient $|R|^2$ at the face of the piston[31], [32].

$$|R|^2 = \left|\frac{Z_{fluid} - Z_{input}^*}{Z_{fluid} + Z_{input}}\right|^2 \quad (14)$$

Here Z_{fluid} is the acoustic radiation impedance of the fluid and Z_{input} is the input impedance of the CPUT in the absence of radiation resistance which can be calculated by obtaining the ratio of the complex force amplitude on the piston to the complex velocity amplitude at the face of the piston ie.

$$Z_{input} = \frac{\bar{F}}{\bar{v}}\Big|_{piston\ surface} \quad (15)$$

Since Z_{fluid} is fixed, CPUT parameters must be optimized to achieve low reflection coefficient in the bandwidth of operation. In the results that follow, Simulink is used to calculate efficiency and reflection coefficient of the example CPUT as a function of various parameters. The analytical solutions are used to complement these results by providing plate displacement, forcing threshold and operational frequency bandwidth data.

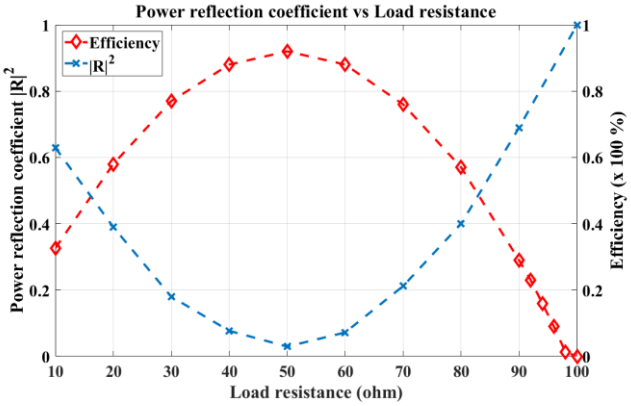

Fig. 3. Power reflection coefficient vs load resistance for a fixed input intensity of 3.33 mW/mm^2. The CPUT efficiency is maximized as the power reflection coefficient is reduced.

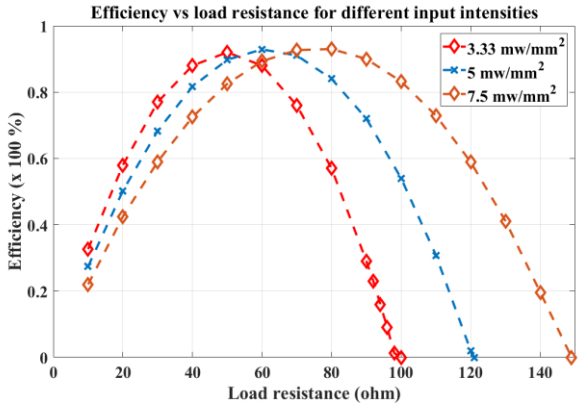

Fig. 4. CPUT efficiency vs load resistance for different input levels of input intensities. A higher input intensity allows a greater critical load resistance ie. The resistance beyond which the system cannot be driven into parametric resonance.

B. Effect of load resistance on efficiency and power reflection coefficient

The input impedance of the CPUT is strongly dependent on the load at the termination. Assuming a purely real load, fig. 3 shows the variation of power reflection coefficient and efficiency with load resistance for a fixed input ultrasound intensity of 3.33 mW/mm^2 at 2MHz (translates to a force of 0.1 N on a piston face having 1mm^2 area) obtained using Simulink. It can be seen that the reflection coefficient which is large at low load resistances, reduces until it reaches a minimum around 50 Ω

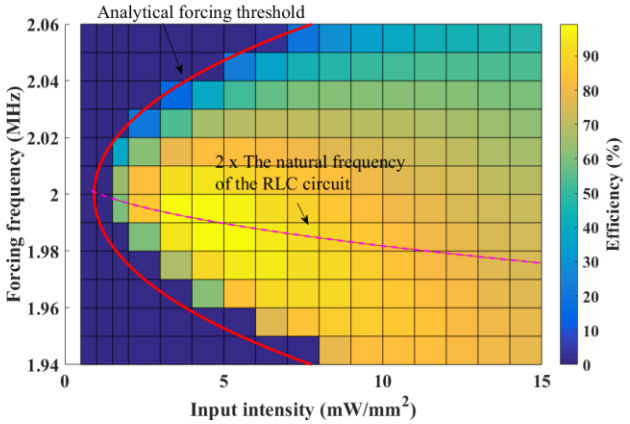

Fig. 5. 2D color map plot of efficiency of the CPUT vs plane wave input intensity and forcing frequency. The solid red line (analytical solution) indicates the operational frequency bandwidth of the CPUT, ie. the region within which the system sustains parametric resonance. The dashed line represents the actual forcing frequency $2w_{oel}'$ required to efficiently drive parametric resonance.

and then increases again until it is maximum at 100 Ω. As expected, a maximum efficiency of over 90% is obtained when the reflection coefficient is minimum. Increasing the load resistance causes Z_{input} to change and the resistance at which maximum efficiency is obtained corresponds to the best impedance match between the CPUT and the fluid medium. At a load resistance of 100 Ω, it is seen that the efficiency drops to zero as the level of ultrasound forcing does not meet the required minimum threshold for parametric resonance as defined in eqn. 12. The upper limit of this critical load resistance can be increased further by increasing the level of

forcing. As shown in fig. 4, if the input intensity level is increased, the range of load resistance in which parametric resonance is obtained, is also increased. It is also observed that the resistance at which maximum efficiency is obtained is shifted to the right which implies that the input impedance of the CPUT depends on the level of forcing.

The effect of a small shift in excitation frequency on the efficiency of the CPUT is studied by varying the input ultrasound intensity and the forcing frequency at a fixed resistance of 50 Ω. Using Simulink, the CPUT efficiency is obtained from input intensities ranging from 1 mW/mm^2 to 15 mW/mm^2. The ultrasound forcing frequency ω_{us} is also varied about its value of 2 MHz to determine the frequency bandwidth of operation. From the resulting 2D plot shown in fig. 5, it can be seen that the operational frequency bandwidth predicted by the analytical solution (solid red line) closely tracks the boundary beyond which parametric resonance is not sustained (indicated by areas of zero efficiency as calculated using Simulink). Interestingly, the maximum efficiency is seen at a frequency slightly lower than $2\omega_{oel}$. This can be explained by the fact that the system is excited into parametric resonance most effectively when the forcing frequency is two times the resonant frequency of the RLC circuit. However, as the input intensity is increased, a larger voltage develops across the capacitor. This in turn leads to a larger average attractive electrostatic force on the piston, thereby increasing the mean displacement y defined in eqn. 10. This causes the capacitance of the capacitor to increase from C_0 to C_0' thereby slightly decreasing the electrical resonance frequency to ω_{oel}'. To efficiently excite the system, the ultrasound frequency should be equal to two times ω_{oel}'. By calculating the change in capacitance using the displacement data from the analytical solution, the actual $2\omega_{oel}'$ is plotted as a dashed line in fig. 5. It is observed that the regions of maximum efficiency on the color plot closely follow this line thereby validating this argument. Looking back at fig. 3 and 4, one can also conclude that a better impedance match and a higher efficiency, reaching closer to 100%, could be obtained if the forcing frequency was ω_{oel}' instead of 2MHz.

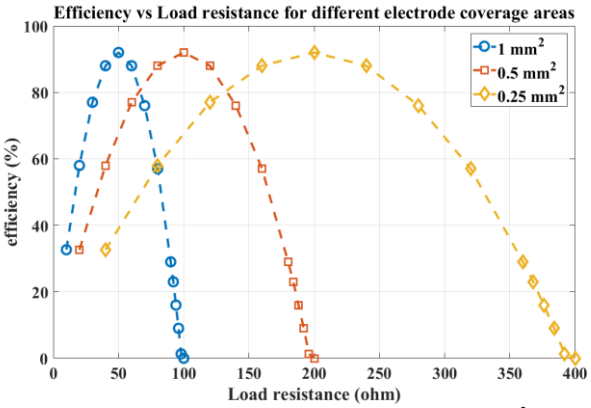

Fig. 6(a). CPUT efficiency for 3 different electrode areas of 1mm^2, 0.5mm^2 and 0.25mm^2 (R=50 Ω and I=3.33 mW/mm^2) The corresponding inductance values used are 343 µH, 686 µH and 1372 µH respectively and the forcing frequency is 2 MHz.

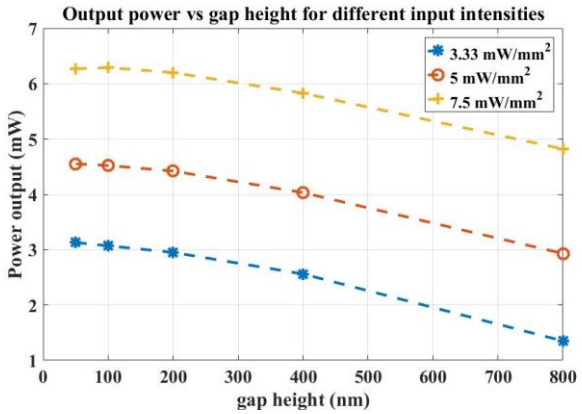

Fig. 6(b). Variation of power output for increasing gap height at different input intensities for R=50 Ω. As the gap height is increased, the operational bandwidth becomes narrower, thus causing the efficiency to drop more rapidly with any variation from $2\omega_{oel}'$

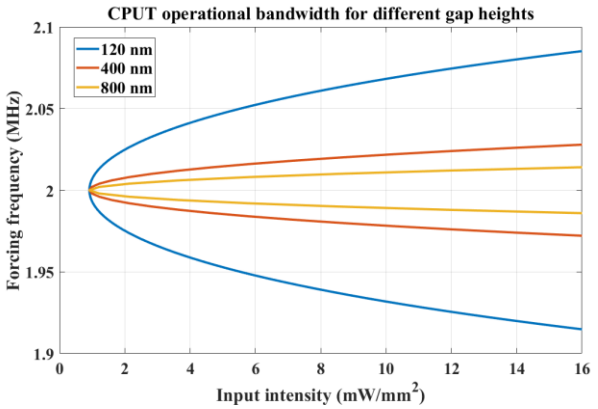

Fig. 6(c). Effect of CPUT gap height on operational frequency bandwidth for R=50 Ω and I=3.33 mW/mm^2. Each solid line represents the frequency limits within which the CPUT sustains parametric resonance. It is seen that increasing the gap height causes narrowing of operational frequency bandwidth of the CPUT.

Using eqn. 12, the minimum input intensity required for different US frequencies is also plotted as a solid line in fig. 5. Due to the resistive loss in the RLC circuit, the apex of the curve is centered at a non-zero input intensity at 2MHz and is symmetric on either side of the center frequency. It can be seen that increasing the input intensity causes the operational frequency bandwidth of the CPUT to broaden. The drop in efficiency when the forcing frequency is slightly different from $2\omega_{oel}'$ is also less drastic at higher levels of input intensity. Thus, in order to operate this example CPUT at the maximum possible efficiency, 3 factors must be considered – (i) the right load resistance for the operational input intensity must be chosen to minimize reflection at the face of the piston. (ii) The forcing frequency must be slightly detuned to $2\omega_{oel}'$ to ensure that the CPUT is efficiently driven into parametric oscillation and (iii) a greater input intensity is required in order to operate the CPUT efficiently over a larger frequency bandwidth.

C. Effect of electrode coverage and gap height on efficiency

The effect of electrode coverage on the CPUT efficiency as obtained using Simulink is shown in fig. 6(a) for a receiver of area 1mm^2 and input intensity of 3.33 mW/mm^2 at 2 MHz. It is

observed that for the same piston area, reducing the area of the electrode has a negligible effect on the CPUT maximum efficiency. When the electrode area is reduced, the force required to sustain parametric resonance (as defined in eqn. 12) decreases. Thus, maintaining the same level of forcing causes the critical load resistance to increase and shifts the point of maximum efficiency to the right. In a real membrane/plate based CPUT, the average displacement is less than the displacement of an equivalent parallel plate piston as the center of the membrane undergoes larger range of motion whereas the regions near the clamped edges don't move as much. By restricting the electrode coverage to the central high deflection zone, we can compensate for the lower average displacement and still obtain a high efficiency. Furthermore, reducing the electrode area for the same operating frequency also increases the range of load resistance and this provides us with more flexibility in terms of matching the CPUT to a wider range of resistive loads.

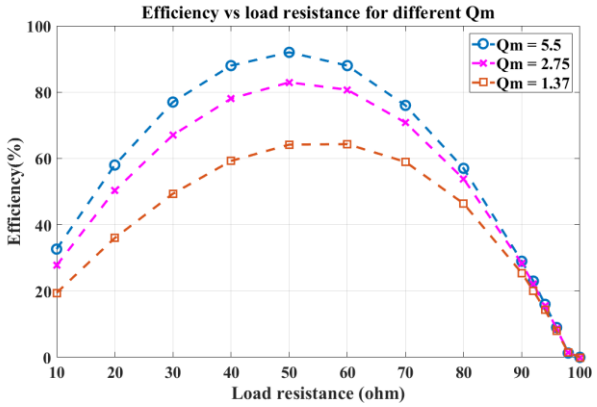

Fig. 7: Change in efficiency as a function of load resistance for a fixed input forcing of 3.33 mW/mm^2 at 2 MHz. The maximum achievable efficiency decreases at mechanical Q factor of the CPUT is reduced.

The flexibility with choosing gap height also needs to be considered while fabricating the CPUT. The variation in output power with increasing gap height at a fixed load resistance of 50 Ω and forcing of 3.33 mW/mm^2 at 2MHz is shown in fig. 6(b). It is observed that increasing the gap height causes the output power to gradually decrease for different input intensities. Unlike the previous case, where decreasing the electrode area increased the critical resistance, the gap height has no such effect. Instead increasing the gap causes the frequency bandwidth of operation to decrease (fig. 6c.). This means that any slight deviation from the actual forcing frequency $2\omega_{oel}'$ causes the CPUT efficiency to drastically decrease. This narrowing of operational bandwidth due to increased gap, when coupled with reduced intensity (which causes further narrowing of operational bandwidth), resulted in an efficiency drop of nearly 50% when the forcing frequency is shifted from 1.995 MHz to 2 MHz in Simulink for a gap of 800 nm and a forcing of 3.33 mW/mm^2). Fortunately, it is possible to accurately control the ultrasound transmission frequency in a practical system. This enables design of CPUTs with different gap heights without compromising on the efficiency.

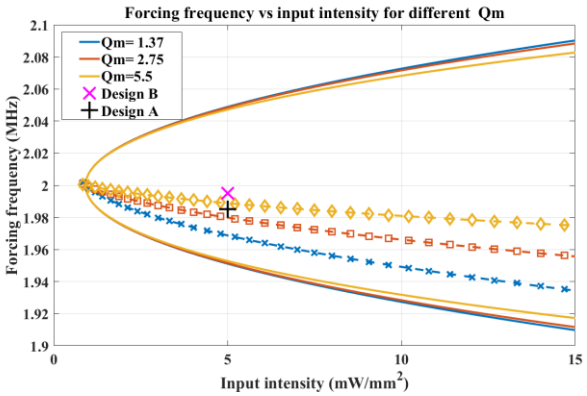

Fig. 8. The parabolic lines indicate the bandwidth of the CPUT for different values of Q_m. The corresponding values of $2\omega_{oel}'$ are indicated by the dashed lines. The location of the two practical designs (design A and B) based on the simulated Q-factor is also marked in the figure.

D. Effect of receiver design on efficiency

The mechanical design of the CPUT receiver is another parameter that must be considered while optimizing CPUT for power transfer applications. The receiver can be made using different structures such as a membrane, stiff plate or interdigitated fingers and from various materials such as silicon, silicon nitride or aluminum. The mechanical Q-factor of the receiver will depend on the choice and shape of material and the fluid of operation. The effect of Q_m on the efficiency of the CPUT driven at 2 MHz at an intensity of 3.33 mW/mm^2 is seen in fig. 7. It is observed that the CPUT having the highest Q_m of 5.5 shows a maximum efficiency of 92%. The maximum achievable efficiency seems to decrease as the Q-factor of the receiver is reduced. This drop in efficiency with reduction of Q-factor is explained using the forcing frequency vs input intensity graph shown in fig. 8. Although the lowering of Q-factor does not affect the operational bandwidth significantly (represented by the parabolic lines), the actual forcing frequency required for efficient parametric resonance $2\omega_{oel}'$, shown by the dashed lines, shifts to a lower frequency as Q-factor is reduced. As explained previously, this indicates that a CPUT with a low-Q factor membrane must be excited at a lower frequency in order to be operated efficiently. By operating at 2MHz, the CPUT is being excited at a frequency that is considerably different from $2\omega_{oel}'$ and hence we see a much lower achievable efficiency. Hence the operating point of the CPUT must be considered while designing the receiver and it may be beneficial to tune it such that the receiver resonance ω_{om} is much closer to $2\omega_{oel}'$ to obtain the best performance. This also provides us with more design flexibility as we can design receivers with different geometries and thicknesses without compromising on efficiency.

IV. PRACTICAL CONSIDERATIONS FOR CPUT OPERATION IN WATER AND AIR

A. Practical CPUT designs for operation in water

To determine the feasibility of realizing a device with similar specifications as the example CPUT, two different receiver designs are simulated using COMSOL multiphysics (COMSOL

inc.) for operation in water. As the aim of the study is to determine if the specs of the example CPUT can be realized within practical dimensions, only the frequency response of the top plate in fluid is simulated. Design A consists of a 190 µm thick single crystal silicon circular plate having an area of cross section equal to 1mm^2. The resonant frequency in water is found to be 2 MHz and the quality factor of the plate is measured to be approximately 3.4. An input forcing intensity of 3.33 mW/mm^2 is applied on the top plate and the peak displacement amplitude measured at the center of the plate is found to be 14.7 nm with an average displacement of 8 nm across the entire surface. For comparison, the displacement obtained by the parallel plate in the 1D model is 10.6 nm for the same input intensity level.

Design B consists of a 260 µm thick single crystal silicon plate of radius 0.5 mm, mass loaded by a 50 µm thick plate of tungsten having radius 0.4 mm. Once again, the dimensions are selected such that the maximum displacement is obtained at 2 MHz. However, the increased mass of the plate produces a sharper resonance peak with a Q-factor of 10.5. By assuming the input intensity to be 5 mW/mm^2, we can compare these two designs with the example CPUT by noting their location in fig. 9. Although both design A and B have a resonance frequency of 2 MHz, design A must be operated at a slightly lower frequency in order to excite parametric resonance most efficiently in the CPUT.

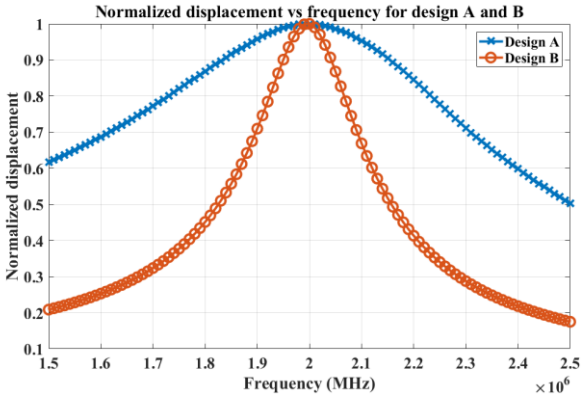

Fig. 9. Normalized displacement as a function of excitation frequency for design A and B as calculated using COMSOL. The additional mass loading in design B leads to a narrower bandwidth and hence a higher Q-factor.

To calculate the value of inductance required for the CPUT, we can assume that the top plate has 100% electrode coverage. Advances in wafer bonding technology [33] enable us to realize small vacuum gaps for large plate area and so we consider the same gap as used for the example CPUT (120 nm) in this realistic design. To obtain an electrical resonance frequency of 1 MHz, a 343 µH inductor is required – this can be easily realized using off the shelf wire-wound inductors. Furthermore, if the electrode area is reduced, the increased inductance can be obtained by connecting the inductors in series. It must be noted that the internal resistance of the inductors add up in series thereby cause a drop in power available across the load resistance. However reducing the electrode area also requires a greater value of load resistance for optimum efficiency as show in fig 6(a), hence care must be taken to ensure that the value of load resistance is much greater than the internal resistance of the inductor in order to maximize output power.

B. Feasibility check for CPUT in air

Technological advances in consumer electronics, wearables and internet-of-things (IoT) have made wireless powering of devices through air a topic of great interest. Recently, Rekhi et.al proposed using pre-charged CMUTs as receivers for wireless powering of nodes using airborne ultrasound [15]. However, pre-charged capacitive receivers may suffer from long-term reliability issues, thus making the CPUT an option for such applications. In this subsection, we evaluate the feasibility of operating the CPUT in air. Using [15] as a basis, the operating ultrasound frequency is selected to be 50 kHz. Since the operation of the CPUT is primarily dependent on driving the system into parametric resonance, it is necessary to ensure that the incident acoustic forcing satisfies the required conditions set by eqn. 12. As per OSHA guidelines [34], the maximum permissible ultrasound intensity in air is limited to 115 dB SPL. This translates to an incident pressure of roughly 16 Pa, which is approximately 4 orders of magnitude lower than that used in the water simulations. However, due to the small acoustic impedance of air as compared to water ($Z_{air} \approx 415$ MRayl) and lower operating frequency, evaluating eqn. 12 reveals that the forcing at 115 dB SPL satisfies the inequality thus indicating that the CPUT works within the specified limits in air.

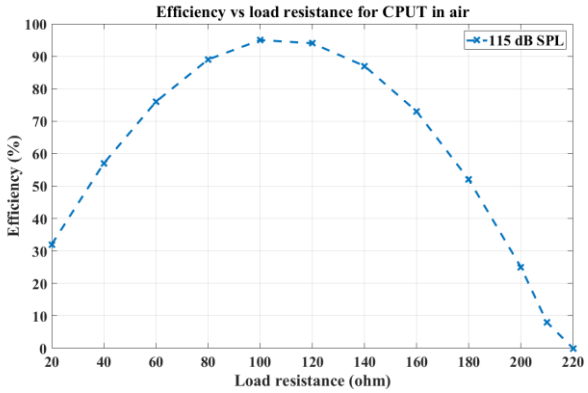

Fig. 10. Efficiency vs load resistance for a CPUT operated in air. The input ultrasound forcing is at 115 dB SPL and 50 kHz.

In order to confirm that the CPUT can indeed be operated in air, COMSOL is first used to design a receiver of area 1.21 cm^2 that resonates at a frequency of 50 kHz. It is found that a receiver consisting of a silicon plate of thickness 1500 µm resonates at 50 kHz with a peak amplitude of 590 nm when subjected to an incident acoustic field of 115 dB SPL. The receiver is also subjected to an average static deflection of approximately 150 nm due to atmospheric pressure. Using the values obtained from COMSOL as a design guideline, an example CPUT with comparable mass and stiffness and a gap of 1.85 µm is simulated using the Simulink model. The vacuum gap is increased to account for both the static deflection due to atmospheric pressure as well as the greater dynamic deflection due to the incident ultrasound field. The efficiency obtained as

a function of load resistance is plotted in fig. 10. The input forcing of 115 dB SPL is clearly sufficient to drive the CPUT into parametric resonance. Moreover, a maximum efficiency of 95% is obtained which is comparable to that achieved by the CPUT in water. Due to the larger gap and lower operating frequency, an inductance of 22.3 mH is required, which is larger than that used for the CPUT in water. Similar to the optimization performed for operation in water, the CPUT can be tailored to operate efficiently in air as a sensor or a power receiver.

V. CONCLUSION

We have presented a 1D lumped parameter model to represent the operation of the CPUT in different media. The operational characteristics of the CPUT were examined by solving the 1D model using Simulink and with the help of analytical solution obtained by solving the coupled non-linear ODEs. Using a set of example parameters, the efficiency of the CPUT was evaluated for different operating parameters such as the load resistance, the frequency of operation, level of input forcing, area of the electrodes and the gap height. It was found that in order to achieve optimum efficiency, the two most important factors to consider are i) to ensure that the impedance of the CPUT is matched as closely to the medium as possible and ii) to drive the CPUT as a frequency slightly lower than $2\omega_{oel}'$ to ensure the most efficient parametric excitation. Two different top plate designs were simulated in COMSOL to confirm that the parameters suggested in the Simulink simulations are practically achievable. Finally, we discussed the feasibility of operating the CPUT in air and showed that although the maximum allowable intensity is many orders of magnitude lower when compared to water, it is still sufficient to induce parametric resonance.

Although the 1D model and analytical expressions presented in this paper is sufficient to explore the basic operating characteristics of a piston-based CPUT, a more involved model similar to that used by Satir et. al [35] will be required to accurately predict system behavior for more complicated cases such as a multi-membrane CPUT. Similarly, the coupling of the CPUT with power recovery circuits needs to be considered. Furthermore, miniaturization of the device is not feasible with the current coil-wound inductors. Employing piezoelectric resonators as inductors [36] is solution worth exploring hence setting a strong platform for further research into air and water power transfer applications using the CPUT.

ACKNOWLEDGEMENT

This work was supported by the ECCS division of the National Science Foundation under the NSF ECCS award no. 1829821.

REFERENCES AND FOOTNOTES

[1] T. L. Szabo, *Diagnostic Ultrasound Imaging: Inside Out*. Academic Press, 2004.

[2] T. A. Ritter, T. R. Shrout, R. Tutwiler, and K. K. Shung, "A 30-MHz piezo-composite ultrasound array for medical imaging applications," *IEEE Trans. Ultrason. Ferroelectr. Freq. Control*, vol. 49, no. 2, pp. 217–230, Feb. 2002.

[3] B. W. Drinkwater and P. D. Wilcox, "Ultrasonic arrays for non-destructive evaluation: A review," *NDT E Int.*, vol. 39, no. 7, pp. 525–541, Oct. 2006.

[4] K. Uchino, "Piezoelectric ultrasonic motors: overview," *Smart Mater. Struct.*, vol. 7, no. 3, p. 273, 1998.

[5] F. L. Degertekin, R. O. Guldiken, and M. Karaman, "Annular-ring CMUT arrays for forward-looking IVUS: transducer characterization and imaging," *IEEE Trans. Ultrason. Ferroelectr. Freq. Control*, vol. 53, no. 2, pp. 474–482, Feb. 2006.

[6] G. Gurun *et al.*, "Single-Chip CMUT-on-CMOS Front-End System for Real-Time Volumetric IVUS and ICE Imaging," *IEEE Trans. Ultrason. Ferroelectr. Freq. Control*, vol. 61, no. 2, pp. 239–250, Feb. 2014.

[7] M. Legros, A. Novell, A. Bouakaz, G. Férin, R. Dufait, and D. Certon, "Tissue harmonic imaging with CMUTs," in *2011 IEEE International Ultrasonics Symposium*, 2011, pp. 2249–2252.

[8] S. H. Wong, M. Kupnik, K. Butts-Pauly, and B. T. Khuri-Yakub, "P1B-10 Advantages of Capacitive Micromachined Ultrasonics Transducers (CMUTs) for High Intensity Focused Ultrasound (HIFU)," in *2007 IEEE Ultrasonics Symposium Proceedings*, 2007, pp. 1313–1316.

[9] Y. Lu *et al.*, "Ultrasonic fingerprint sensor using a piezoelectric micromachined ultrasonic transducer array integrated with complementary metal oxide semiconductor electronics," *Appl. Phys. Lett.*, vol. 106, no. 26, p. 263503, Jun. 2015.

[10] Y. Qiu *et al.*, "Piezoelectric Micromachined Ultrasound Transducer (PMUT) Arrays for Integrated Sensing, Actuation and Imaging," *Sensors*, vol. 15, no. 4, pp. 8020–8041, Apr. 2015.

[11] D. E. Dausch, K. H. Gilchrist, J. B. Carlson, S. D. Hall, J. B. Castellucci, and O. T. von Ramm, "In vivo real-time 3-D intracardiac echo using PMUT arrays," *IEEE Trans. Ultrason. Ferroelectr. Freq. Control*, vol. 61, no. 10, pp. 1754–1764, Oct. 2014.

[12] M. S. Salim, M. F. Abd Malek, R. B. W. Heng, K. M. Juni, and N. Sabri, "Capacitive Micromachined Ultrasonic Transducers: Technology and Application," *J. Med. Ultrasound*, vol. 20, no. 1, pp. 8–31, Mar. 2012.

[13] K. Agarwal, R. Jegadeesan, Y. X. Guo, and N. V. Thakor, "Wireless Power Transfer Strategies for Implantable Bioelectronics: Methodological Review," *IEEE Rev. Biomed. Eng.*, vol. PP, no. 99, pp. 1–1, 2017.

[14] J. S. Ho, S. Kim, and A. S. Y. Poon, "Midfield Wireless Powering for Implantable Systems," *Proc. IEEE*, vol. 101, no. 6, pp. 1369–1378, Jun. 2013.

[15] A. S. Rekhi, B. T. Khuri-Yakub, and A. Arbabian, "Wireless Power Transfer to Millimeter-Sized Nodes Using Airborne Ultrasound," *IEEE Trans. Ultrason. Ferroelectr. Freq. Control*, vol. PP, no. 99, pp. 1–1, 2017.

[16] A. Arbabian *et al.*, "Sound Technologies, Sound Bodies: Medical Implants with Ultrasonic Links," *IEEE Microw. Mag.*, vol. 17, no. 12, pp. 39–54, Dec. 2016.

[17] S. Ozeri and D. Shmilovitz, "Ultrasonic transcutaneous energy transfer for powering implanted devices," *Ultrasonics*, vol. 50, no. 6, pp. 556–566, May 2010.

[18] J. Charthad, M. J. Weber, T. C. Chang, and A. Arbabian, "A mm-Sized Implantable Medical Device (IMD) With Ultrasonic Power Transfer and a Hybrid Bi-Directional Data Link," *IEEE J. Solid-State Circuits*, vol. 50, no. 8, pp. 1741–1753, Aug. 2015.

[19] M. J. Weber, A. Bhat, T. C. Chang, J. Charthad, and A. Arbabian, "A miniaturized ultrasonically powered programmable optogenetic implant stimulator system," in *2016 IEEE Topical Conference on Biomedical Wireless Technologies, Networks, and Sensing Systems (BioWireleSS)*, 2016, pp. 12–14.

[20] J. Knight, J. McLean, and F. L. Degertekin, "Low temperature fabrication of immersion capacitive micromachined ultrasonic transducers on silicon and dielectric substrates," *IEEE Trans. Ultrason. Ferroelectr. Freq. Control*, vol. 51, no. 10, pp. 1324–1333, Oct. 2004.

[21] U. Bartsch, J. Gaspar, and O. Paul, "A 2D Electret-Based Resonant Micro Energy Harvester," in *IEEE 22nd International Conference on Micro Electro Mechanical Systems, 2009. MEMS 2009*, 2009, pp. 1043–1046.

[22] S. Surappa, S. Satir, and F. Levent Degertekin, "A capacitive ultrasonic transducer based on parametric resonance," *Appl. Phys. Lett.*, vol. 111, no. 4, p. 043503, Jul. 2017.

[23] A. P. Seyranian, "The swing: Parametric resonance," *J. Appl. Math. Mech.*, vol. 68, no. 5, pp. 757–764, Jan. 2004.

[24] Y. Jia, J. Yan, K. Soga, and A. A. Seshia, "Parametric resonance for vibration energy harvesting with design techniques to passively reduce

the initiation threshold amplitude," *Smart Mater. Struct.*, vol. 23, no. 6, p. 065011, 2014.

[25] N. B. Caldwell and M. F. Daqaq, "Exploiting the principle parametric resonance of an electric oscillator for vibratory energy harvesting," *Appl. Phys. Lett.*, vol. 110, no. 9, p. 093903, Feb. 2017.

[26] L. E. Kinsler, A. R. Frey, A. B. Coppens, and J. V. Sanders, *Fundamentals of Acoustics, 4th Edition*. 1999.

[27] M. Tao and H. Owhadi, "Temporal homogenization of linear ODEs, with applications to parametric super-resonance and energy harvest," *Arch. Ration. Mech. Anal.*, vol. 220, no. 1, pp. 261–296, 2016.

[28] M. Tao, "Simply improved averaging for coupled oscillators and weakly nonlinear waves," *ArXiv180607947 Phys.*, Jun. 2018.

[29] J. Murdock, J. A. Sanders, and F. Verhulst, "Averaging Methods in Nonlinear Dynamical Systems," *Appl Math Sci*, vol. 59, 2007.

[30] U. F. and D. Administration, "Information for manufacturers seeking marketing clearance of diagnostic ultrasound systems and transducers," *Rockv. MD Cent. Devices Radiol. Health US Food Drug Adm.*, 1997.

[31] M. G. L. Roes, J. L. Duarte, M. A. M. Hendrix, and E. A. Lomonova, "Acoustic Energy Transfer: A Review," *IEEE Trans. Ind. Electron.*, vol. 60, no. 1, pp. 242–248, Jan. 2013.

[32] T. E. G. Álvarez-Arenas, "Acoustic impedance matching of piezoelectric transducers to the air," *Ultrason. Ferroelectr. Freq. Control IEEE Trans. On*, vol. 51, no. 5, pp. 624–633, 2004.

[33] I. O. Wygant *et al.*, "50 kHz capacitive micromachined ultrasonic transducers for generation of highly directional sound with parametric arrays," *IEEE Trans. Ultrason. Ferroelectr. Freq. Control*, vol. 56, no. 1, pp. 193–203, Jan. 2009.

[34] "OSHA Technical Manual (OTM) | Section III: Chapter 5 - Noise | Occupational Safety and Health Administration." [Online]. Available: https://www.osha.gov/dts/osta/otm/new_noise/#appendixc. [Accessed: 23-Jan-2018].

[35] S. Satir, J. Zahorian, and F. L. Degertekin, "A large-signal model for CMUT arrays with arbitrary membrane geometry operating in non-collapsed mode," *Ultrason. Ferroelectr. Freq. Control IEEE Trans. On*, vol. 60, no. 11, pp. 2426–2439, 2013.

[36] B. Ju, W. Shao, L. Zhang, H. Wang, and Z. Feng, "Piezoelectric ceramic acting as inductor for capacitive compensation in piezoelectric transformer," *IET Power Electron.*, vol. 8, no. 10, pp. 2009–2015, 2015.